DUST PLUMES LOFTED BY SLIDING CO_2 ICE BLOCKS, RUSSELL MEGADUNE, MARS. C. L. Dinwiddie[1] and T. N. Titus[2], [1]Space Science and Engineering Division, Southwest Research Institute®, San Antonio, Texas, cdinwiddie@swri.org, [2]U.S. Geological Survey, Astrogeology Science Center, Flagstaff, Arizona, ttitus@usgs.gov.

Introduction: The formation of linear dune gullies on poleward-facing Martian slopes by CO_2-ice block or snow-cornice falls has been proposed [1–3] based on optical imagery of bright, discrete, high-albedo features resting inside gully channels. Because bright features inside gully channels can resemble patchy frost rather than three-dimensional blocks, we provide additional evidence from the Russell crater megadune (54.2°S, 12.8°E) to support the ice-block formation hypothesis for linear dune gullies. We identified four HiRISE or CTX camera images acquired of four airborne dust plumes with in-channel sources, thrust up and dispersed outward along the paths of megadune gullies [4]. Two plumes lofted at solar longitude (L_s) 202° are observed in CTX image J06_047078_1253 (**Fig. 1**), and part of the near-field plume is observed in HiRISE image ESP_047078_1255. HiRISE image PSP_002904_1255 and CTX image D06_029408_1254 also capture similar dust plumes lofted at L_s 197° and 200° (Fig. 1). The narrow L_s window when this activity is observed suggests that it is seasonal. We show how these dust plumes are lofted by ice blocks sliding down linear dune gullies, and that this activity redistributes silt and dust, resulting in seasonal variable-albedo patterns on the lee slope of the megadune. We use optical and spectral imaging, a digital terrain model, and observation-validated thermal modeling to develop a mechanistic framework for linear dune gully formation [4].

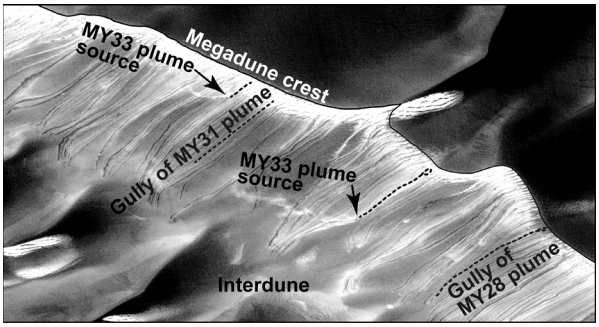

Fig. 1. *CTX J06_047078_1253 captured two simultaneous airborne dust plumes with in-channel sources on the megadune at L_s 202° in Mars Year (MY) 33; gullies associated with two other earlier dust plumes are also indicated.*

Site Characterization: CO_2 frost first condenses on the megadune between L_s 30° and 40°, initially on the steepest, poleward-facing slopes on which the thickest deposits accumulate and persist into mid-spring [4]. We estimate CO_2 ice thickness on the megadune, as a function of L_s and slope angle [4] using the KRC thermal model [5]. By the time afternoon daylight returns to the scene (as early as L_s 105°), faint Dark Dune Spots {DDS; [6]} appear on crests of superimposed secondary dunes on the stoss slope of the megadune [4]. When DDS first appear (i) 16-to-36-cm-thick ice has accumulated {modeling assumed 1,000 kg/m^3 CO_2 ice density}, (ii) estimated basal heat flux is <1.9 W/m^2, and (iii) peak insolation absorbed by the ice ranges from 0 W/m^2 on slopes >11.4° to ~60 W/m^2 on flat plains [4]. By L_s 115°, the quantity of DDS markedly increases when (i) 20-to-41-cm-thick ice has accumulated, (ii) estimated basal heat flux has declined to <1.4 W/m^2, and (iii) peak insolation absorbed by the ice ranges from 0 W/m^2 on slopes >10° to ~78 W/m^2 on flat plains [4].

From L_s 105° to 157°, a polygonal crack network is visible in low-albedo, translucent CO_2 ice, potentially representing local zones of weakness [4]. Thereafter, increasing insolation and ice brightening conceal polygonal cracks, but araneiform troughs become more visible [4]. DDS and associated dendritic, araneiforms [7, 8], or furrows [9] are thought to mark vents of high-pressure CO_2 gas jets {i.e., Kieffer's jets; [10–12]} at weak spots in the CO_2 ice. CO_2 gas forms at the ice–dune interface from either basal heat flux-induced or insolation-induced basal sublimation (IIBS) of the translucent ice [13, 14]. Kieffer [15] provides a detailed description of this venting process, which produces DDS or dark fan-shaped deposits of sand above ice [16]. *By* L_s 136°, DDS vents produce channelized, gravitational flows of dark sand when ice is >0.4-m-thick [4]. Pilorget and Forget [10] suggest that sediment jets recur repeatedly from DDS vents each season and result in fluidized, viscous debris flows, perhaps beneath slab ice. CO_2 gas likely erodes dune sand during transport to DDS vents, and dendritic, araneiform troughs and downslope flows may rework the dune surface and carve small tributary channels that merge downslope into the linear dune gullies [4]. DDS vents form at the same positive-relief locations each season, indicating a positive-feedback mechanism such that they are a self-reinforcing phenomenon [4]. All CO_2 ice sublimates by L_s 217°, but araneiforms and positive-relief knobs on which DDS vents form remain visible [4]; the knobs may be sand deposits transported to vents by CO_2 gas, but not ejected during venting [4].

CO_2 Ice Block Formation & Dust Content: From L_s 157° to 202°, our model predicts condensed CO_2 ice thickness of ~0.50 m on the steepest slopes. Alcoves at the megadune crest also collect windblown CO_2 snow. Snow morphs into porous ice on Mars [17–19], so seasonal ice within alcoves (directly condensed + metamorphosed snow) may be several meters thick. We measured 1.5- to 5-m CO_2 ice blocks in megadune gullies, indicating even larger blocks detach from their point of

origin and slide downhill [4]. We hypothesize that thermal power from IIBS rather than basal heat flux primarily drives jets of CO_2 gas through DDS vents, ultimately fragmenting slab ice and dislodging ice blocks by L_s 197° through vigorous agitation of the polygonal crack network [4]. Atmospheric dust forms condensation nuclei for CO_2 snow on Mars. Assuming an atmospheric dust-to-gas mixing ratio of 7.5×10^{-6} [15] and CO_2-ice density of 1,000 kg/m^3 [13, 19–23], dust abundance in a 2-m-thick ice block is 15 μm/m^2 [4]. By L_s 202°, the megadune accumulates a coarse silt/dust layer of sublimation-lag residue that is a few microns thick [4].

CO_2 Ice Block and Dust Mobility: Gas pressure from IIBS dislodges ice blocks near the megadune crest, the blocks fall from steep terrain, and funnel into linear dune gullies [4]. As dust is mobilized by ice blocks, fine grains are lofted into suspension, forming optically thick, narrow dust plumes that are dispersed downwind [4]. Although the plumes obscure their mobile ice block sources, the narrowness of the plumes inside gullies indicates ice-block point sources [4]. We dismiss an interpretation that early spring airborne dust plumes are a manifestation of local DDS venting [24], because the required slab ice has already sublimed from dune slopes where these plumes originate [4].

Gas pressure from subliming ice blocks redistributes sublimation lag, removing coarse silt from channel levees and depositing fine silt around active channels [4]. Dark gully fringes develop when sliding, off-gassing ice blocks throw sand out of channels via saltation and onto levees, burying bright sublimation lag beneath dark sand [4]. Bright gully fringes develop when saltating coarse silt driven by off-gassing ice blocks deposits farther from the channel; locally thick silt deposits form adjacent active gullies, visible as an intermediate-albedo fringe in optical data [4].

CO_2 Ice Block Fate: Ice blocks settle to rest when gas lubrication is no longer sufficient to overcome friction, such as when the slope flattens. Subliming blocks at rest continue to redistribute coarse silt, and add their own embedded dust to their surroundings in an intermediate-albedo dust fringe [4]. Multiple ice blocks resting near the terminus of gullies within dust-plume imagery (e.g., ESP_047078_1255) provide additional support to the interpretation of these airborne dust plumes [4]. When an ice block is dislodged, its surface can become thermally stressed due to an abrupt change in surface thermal gradient [25] or increased insolation [26]. Translucent CO_2 ice fractures and brightens due to increased internal light scattering, and brightening reduces the sublimation rate, increasing the longevity of resting ice blocks. As ice blocks sublimate, they temporarily leave a patchy frost residue [4].

Conclusions: CO_2 ice blocks are an agent of change on the Russell crater megadune that actively modify the dune surface, alter linear dune gullies, and redistribute coarse-grained dust and silt (seasonal sublimation lag). IIBS and CO_2 gas venting cause CO_2-ice-block or snow cornice detachment, falls, and slides from steep near-crest slopes during early spring, accompanied by off-gassing and saltation of sand and coarse silt that is redeposited around gully channels, as well as loft sublimation lag into the observed airborne plumes. Redistribution of seasonal sublimation lag by sliding, subliming ice blocks explains many observed seasonal albedo features on the lee slope of the megadune. Image observations and modeling strongly support the likelihood that this uniquely Martian process is responsible for many of the seasonal albedo variations observed on the lee slope, as well as on smaller dunes within Russell crater.

Acknowledgments: This research was funded by the NASA Mars Data Analysis Program, Grant No. 80NSSC19K1595 (Dinwiddie) and interagency transfer 80HQTR19T0103 (Titus). This research was published in full by *GRL 48*(6) [4] in February 2021. We used JMARS to identify Russell dune field imagery and data (jmars.asu.edu/). These data are available through the Planetary Data System and are found using cited images (pds-geosciences.wustl.edu/ and viewer.mars.asu.edu/). Access KRC thermal modeling code via links in KRC Wiki (krc.mars.asu.edu/).

References: [1] Dundas C. M. *et al.* (2012) *Icarus, 220* (1), 124–143. [2] Diniega S. *et al.* (2013) *Icarus, 225* (1), 526–537 [3] Dundas C. M. *et al.* (2019) *Martian Gullies and Their Earth Analogs, 467,* 67–94. [4] Dinwiddie C. L. and Titus T. N. (2021) *GRL, 48,* e2020GL091920. [5] Kieffer H. H. (2013) *JGR–Planets, 118* (3), 451–470. [6] Mangold N. *et al.* (2003) *JGR–Planets, 108* (E4), 5027. [7] Gardin E. *et al.* (2010) *JGR–Planets, 115* (E6), E06016. [8] Portyankina G. *et al.* (2017) *Icarus, 282,* 93–103. [9] McKeown L. E. *et al.* (2017) *Scientific Reports, 7,* 14181. [10] Pilorget C. and Forget F. (2016) *Nature Geosci., 9,* 65–69. [11] Piqueux S. and Christensen P. R. (2008) *JGR–Planets, 113,* E06005. [12] Portyankina G. (2014) *Encyclopedia of planetary landforms,* 1–7. NYC: Springer. [13] Aharonson O. (2004) *LPS XXXV,* Abstract #1918. [14] Hansen C. J. *et al.* (2010) *Icarus, 205,* 283–295. [15] Kieffer H. H. (2007) *JGR–Planets, 112* (E8), E08005. [16] Malin M. C. and Edgett K. S. (2001) *JGR–Planets, 106,* 23429–23570. [17] Cornwall, C. and Titus T. N. (2009) *JGR–Planets, 114,* E02003. [18] Cornwall C. and Titus T. N. (2010) *JGR–Planets, 115,* E06011. [19] Mount C. P. and Titus T. N. (2015) *JGR–Planets, 120,* 1252–1266. [20] Haberle R. M. *et al.* (2004) *GRL, 31,* L05702. [21] Kieffer H. H. *et al.* (2000) *JGR–Planets, 105,* 9653–9699. [22] Matsuo H. and Heki K. (2009) *Icarus, 202,* 90–94. [23] Smith D. E. *et al.* (2001) *Science, 294,* 2141–2145. [24] Hansen C. J. *et al.* (2020) *LPS LI,* Abstract #2351. [25] Kieffer H. H. (1968) CalTech Ph.D. Dissertation. [26] Paige D. A. and Ingersoll A. P. (1985) *Science, 228,* 1160–1168.